

Thermodynamics Drives the Stability of the MOF-74 Family in Water

Albert A. Voskanyan, Vitaliy G. Goncharov, Novendra Novendra, Xiaofeng Guo, and Alexandra Navrotsky*



Cite This: *ACS Omega* 2020, 5, 13158–13163



Read Online

ACCESS |



Metrics & More

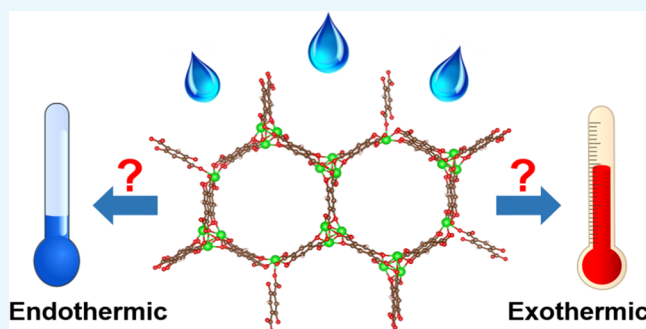


Article Recommendations



Supporting Information

ABSTRACT: The stability of functional materials in water-containing environments is critical for their industrial applications. A wide variety of metal–organic frameworks (MOFs) synthesized in the past decade have strikingly different apparent stabilities in contact with liquid or gaseous H₂O, ranging from rapid hydrolysis to persistence over days to months. Here, we show using newly determined thermochemical data obtained by high-temperature drop combustion calorimetry that these differences are thermodynamically driven rather than primarily kinetically controlled. The formation reaction of a MOF from metal oxide (MO) and a linker generally liberates water by the reaction MO + linker = MOF + H₂O. Newly measured enthalpies of formation of Mg-MOF-74_(s) + H₂O_(l) and Ni-MOF-74_(s) + H₂O_(l) from their crystalline dense components, namely, the divalent MO (MgO or NiO) and 2,5-dihydroxyterephthalic acid, are 303.9 ± 17.2 kJ/mol of Mg for Mg-MOF-74 and 264.4 ± 19.4 kJ/mol of Ni for Ni-MOF-74. These strongly endothermic enthalpies of formation indicate that the reverse reaction, namely, the hydrolysis of these MOFs, is highly exothermic, strongly suggesting that this large thermodynamic driving force for hydrolysis is the reason why the MOF-74 family cannot be synthesized via hydrothermal routes and why these MOFs decompose on contact with moist air or water even at room temperature. In contrast, other MOFs studied previously, namely, zeolitic imidazolate frameworks (ZIF-zni, ZIF-1, ZIF-4, Zn(CF₃Im)₂, and ZIF-8), show enthalpies of formation in the range 20–40 kJ per mole of metal atom. These modest endothermic enthalpies of formation can be partially compensated by positive entropy terms arising from water release, and these materials do not react appreciably with H₂O under ambient conditions. Thus, these differences in reactivity with water are thermodynamically controlled and energetics of formation, either measured or predicted, can be used to assess the extent of water sensitivity for different possible MOFs.



INTRODUCTION

Metal–organic frameworks (MOFs) are a fascinating class of crystalline porous materials, constructed from the coordination of inorganic metal nodes and organic linkers.^{1–3} Their potential functionalities, topologies, and physicochemical properties can be readily tuned by choosing appropriate components in the process of MOF assembly through the reticular chemistry approach.^{4,5} As a result, a library of nanoporous MOF materials with ultrahigh specific surface areas, tailored pore sizes, and mechanical properties has been successfully synthesized, members of which have demonstrated great promise for various applications including gas storage and separation, sensing, drug delivery, catalysis, and energy storage.^{6–10} However, though MOFs possess extremely high surface areas compared to zeolites and activated carbons, many show limited hydrothermal stability.^{11–13} This significantly hinders their practical applications because H₂O is commonly present in different forms in industrial processes. Thus, to prevent undesirable hydrolysis reactions, different strategies have been employed, including, but not limited to, constructing carboxylate MOFs with high valence metal

cations,¹⁴ building azolate frameworks with nitrogen-donor ligands,¹⁵ and functionalizing pore walls with hydrophobic groups.¹⁶ Despite great progress in fabricating MOFs with enhanced water stability, producing highly water/moisture stable MOFs still remains a daunting task. Therefore, it is imperative to explore the thermodynamic stability of MOFs in the presence of water.

Specifically, the present work seeks to answer whether water sensitivity for the MOF-74 family is driven by thermodynamics or controlled by kinetic factors. For initial thermodynamic analysis, we chose the MOF-74 family because of its wide recognition, particularly Mg-MOF-74 is known as one of the best candidates for the efficient postcombustion CO₂ capture from water-containing flue gas generated from coal-fired power

Received: March 17, 2020

Accepted: May 12, 2020

Published: May 26, 2020



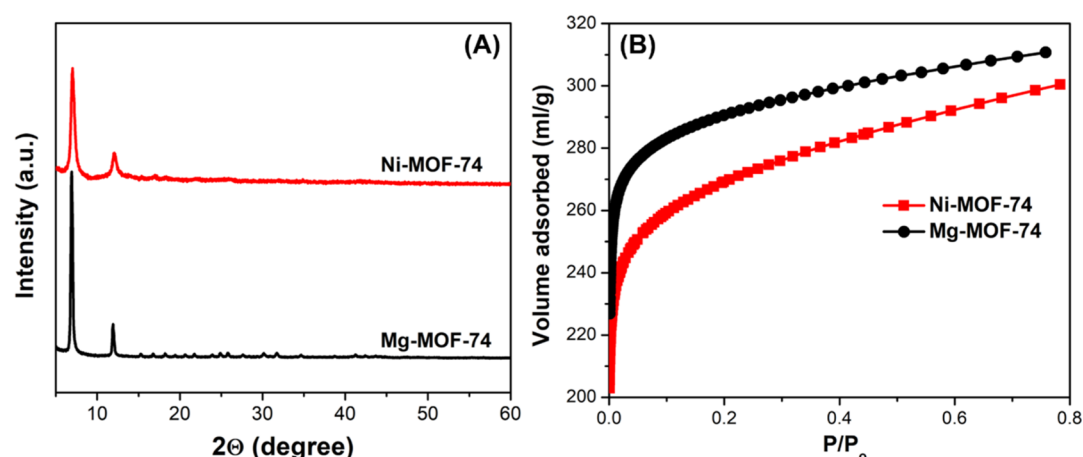


Figure 1. (A) PXRD patterns and (B) N_2 sorption isotherms of Mg-MOF-74 and Ni-MOF-74.

plants.^{17,18} In contrast to other carboxylate MOFs, the MOF-74 family is very water-sensitive, thus it provides a good test of the importance of thermodynamic factors in determining MOF stability in the presence of water.

This work reports the first experimental study of the thermodynamic stability of water-sensitive MOFs using high-temperature drop combustion calorimetry. Unlike traditional room temperature acid or base solution calorimetry where the thermochemical parameters of MOFs are calculated from the measured heats of dissolutions,^{19–21} the new methodology utilizes the heats of combustions at elevated temperature without any solvent. By using a specially designed dropping device developed initially for the study of actinide materials,²² the activated samples can be kept in a totally water-free environment throughout the experiment. Importantly, drop combustion calorimetry allows the investigation of the thermodynamic properties of MOFs, which are not soluble or have limited solubility in acid or base solution at room temperature, hence dramatically extending the scope of MOF choice, including the MOF-74 family. Both methods have their merits. Complete solubility of the sample can be an issue in room temperature solution calorimetry, because incomplete dissolution or unexpected side reactions in the solvent may significantly affect the measured heat effect. Drop combustion calorimetry avoids this problem because of the high temperature and oxygen atmosphere, which convert organic–inorganic materials into metal oxide (MO), CO_2 , and H_2O . However, unlike the large heat effects of drop combustion calorimetry, the heat effects of solution calorimetry are much smaller, and hence the presence of possible impurities can have less impact on the recorded heat. Thus, combustion calorimetry needs to be carried out very carefully and with well-characterized samples. This study paves the way for the thermochemical study of a much larger variety of MOFs, which will facilitate fundamental understanding and guide rational design and fabrication of MOFs with higher hydrothermal stability.

RESULTS AND DISCUSSION

The isostructural Mg-MOF-74 and Ni-MOF-74 were synthesized according to the established protocols from the literature with details given in the experimental section. Powder X-ray diffraction (PXRD) was used to confirm the phase purity of the materials as shown in Figure 1A. Both samples have diffractograms well matching those of Mg-MOF-74 and Ni-

MOF-74 reported in the literature.²³ The porosity was analyzed by N_2 physisorption measurements (Figure 1B). As expected, both materials show typical type-I sorption isotherms with sharp N_2 uptake at very low pressures, indicative of the microporous structure. The calculated Brunauer–Emmett–Teller (BET) surface areas are 1141 and 956 m^2/g and give pore volumes of 0.49 and 0.47 mL/g for Mg-MOF-74 and Ni-MOF-74, respectively. The obtained surface areas are within the range reported in the literature and indicate high purity of the samples. For example, 940 m^2/g was reported for Mg-MOF-74 and 941 m^2/g for Ni-MOF-74.^{24,25} The metal to ligand stoichiometry was confirmed by thermogravimetric analysis (TGA) in O_2 (Figure S1). The weight loss was calculated from 250 to 600 $^{\circ}C$ and corresponds to 2:1 metal/ligand molar ratio within ± 5 wt % uncertainty.

The heats of combustion (ΔH_{com}) of the activated MOFs and their corresponding ligand, 2,5-dihydroxyterephthalic acid (H_4DOBD), were measured at 800 $^{\circ}C$ in O_2 . The MOF completely oxidizes to a MO (MgO or NiO), and gaseous CO_2 , and H_2O . Using an appropriate thermochemical cycle (Table 1) and the measured ΔH_{com} values (Table 2), the enthalpy of reaction (ΔH_r°) between MO (M = Mg or Ni) and H_4DOBD ligands forming the M-MOF-74 and H_2O (liquid) at room temperature was determined. The obtained

Table 1. Thermochemical Cycle Used to Calculate the Enthalpy of Reaction at Room Temperature (ΔH_r°) between MO (M = Mg or Ni) and H_4DOBD Ligand Forming the M-MOF-74 and H_2O via High-Temperature Drop Combustion Calorimetry at 800 $^{\circ}C$ in O_2 ^a

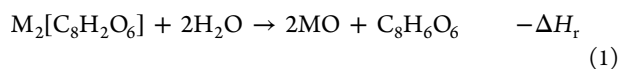
reactions used in the thermochemical cycle	enthalpy
$M_2[C_8H_2O_6]_{(s,25^{\circ}C)} + 6.5O_{2(g,800^{\circ}C)} \rightarrow 2MO_{(s,800^{\circ}C)} + 8CO_{2(g,800^{\circ}C)} + H_2O_{(g,800^{\circ}C)}$	$\Delta H_1 = \Delta H_{com}(MOF-74)$
$C_8H_6O_6_{(s,25^{\circ}C)} + 6.5O_{2(g,800^{\circ}C)} \rightarrow 8CO_{2(g,800^{\circ}C)} + 3H_2O_{(g,800^{\circ}C)}$	$\Delta H_2 = \Delta H_{com}(H_4DOBD)$
$MO_{(s,25^{\circ}C)} \rightarrow MO_{(s,800^{\circ}C)}$	$\Delta H_3 = H_{800}^{\circ} - H_{25}^{\circ}$
$H_2O_{(l,25^{\circ}C)} \rightarrow H_2O_{(g,800^{\circ}C)}$	$\Delta H_4 = H_{800}^{\circ} - H_{25}^{\circ}$
$2MO_{(s,25^{\circ}C)} + C_8H_6O_6_{(s,25^{\circ}C)} \rightarrow M_2[C_8H_2O_6]_{(s,25^{\circ}C)} + 2H_2O_{(l,25^{\circ}C)}$	$\Delta H_r^{\circ} = 2\Delta H_3 + \Delta H_2 - \Delta H_1 - 2\Delta H_4$

^a ΔH_1 and ΔH_2 are experimentally measured and their values are listed in Table 2, ΔH_3 and ΔH_4 are the heat contents of MO and H_2O at 800 $^{\circ}C$ and their corresponding values can be found in ref 35.

Table 2. Thermodynamic Data Obtained by High-Temperature Drop Combustion Calorimetry Measurements at 800 °C in O₂

compound	formula	ΔH_{com} (kJ/mol formula)	$\Delta H_{\text{r}}^{\circ}$ (kJ/mol of M)	$H_{800}^{\circ} - H_{25}^{\circ}$ (kJ/mol)
Mg-MOF-74	Mg ₂ [C ₈ H ₂ O ₆]	-3079.9 ± 16.44	303.89 ± 17.21	
Ni-MOF-74	Ni ₂ [C ₈ H ₂ O ₆]	-2989.9 ± 18.76	264.38 ± 19.44	
H ₄ DOBDC	C ₈ H ₆ O ₆	-2394.0 ± 5.12		
MgO	MgO			34.24
NiO	NiO			39.73
H ₂ O	H ₂ O			73.30
ZIF-1	C ₆ H ₆ N ₄ Zn		19.9 ± 2.5 ³⁷	
ZIF-4	C ₆ H ₆ N ₄ Zn		22.1 ± 2.7 ³⁷	
ZIF-7	C ₁₄ H ₁₀ N ₄ O _{2.24} Zn		27.2 ± 3.9 ³⁷	
ZIF-8	C ₈ H ₁₀ N ₄ Zn		27.1 ± 1.9 ³⁷	
qtz-Zn(CF ₃ Im) ₂	C ₇ H ₆ N ₄ F ₃ Zn		27.1 ± 1.0 ⁴¹	
SOD-Zn(CF ₃ Im) ₂	C ₇ H ₆ N ₄ F ₃ Zn		42.7 ± 1.1 ⁴¹	

values of $\Delta H_{\text{r}}^{\circ}$ are 303.9 ± 17.2 and 264.4 ± 19.4 (kJ/mol of M) for Mg-MOF-74 and Ni-MOF-74, respectively. Mg-MOF-74 is slightly more energetically unstable than Ni-MOF-74. These positive values indicate that the formation of M-MOF-74 plus liquid H₂O from oxide and linker is strongly endothermic, which directly means the reverse reaction of MOF-74 and H₂O (eq 1) is highly exothermic. The exothermic reaction suggests the metastability of the MOF with respect to hydrolysis



The release of H₂O in the formation reaction and its consumption during hydrolysis will make a small entropic $T\Delta S$ contribution to the free energy of reaction. The enthalpic contribution especially at room temperature and with liquid water as a reference state is by far the larger term, so the free energy of reaction is dominated by ΔH . The persistence of a phase under potential reaction conditions is governed by an interplay between thermodynamic driving forces (negative free energy of reaction) and kinetic barriers. In general, the larger the thermodynamic driving force the more likely the system is to overcome any potential kinetic barrier to reaction. Thus, given the very large exothermic driving forces for hydrolysis, it is not surprising that the two MOF-74 samples degrade in the presence of water.

In a fully dehydrated state, the metal nodes in the MOF-74 structure are coordinated with the five oxygen atoms of carboxyl and hydroxy groups of the ligand, leaving one coordinatively unsaturated metal site, which was originally occupied by water or solvent molecules. The formed structure with **etb** topology creates unimodal ~ 1.1 nm hexagonal pores composed of square-pyramidal metal-oxide clusters forming the vertices of the pores. The exposed coordinatively unsaturated metal atoms, which serve as Lewis acid sites, are known to strongly bind with Lewis bases, such as H₂O and CO₂ molecules with remarkably high uptake at room temperature and low partial pressures,^{26,27} which is supported by our thermodynamic results. This means that the interaction of water molecules with MOF-74 is strongly thermodynamically driven and not simply a matter of kinetics.

Because of such a high water affinity, Mg-MOF-74 undergoes structural changes or chemical transformations when exposed to water at ambient temperatures.^{28–30} Specifically, it has been demonstrated that though Mg-MOF-74 exhibits superior adsorption capacity for CO₂ in dry flue gas, the CO₂ capacity was dramatically decreased to 16% of the

initial capacity after exposure at 70% relative humidity (RH).²⁶ Furthermore, after 1 day of exposure at 75% RH, the surface area of Mg-MOF-74 decreased by 74% and after 14 days was only 6 m²/g.³¹ This may suggest some irreversible decomposition on water exposure. Although the XRD pattern may still show some retention of the original MOF diffraction peaks, the loss of surface area strongly supports partial structural collapse and amorphization. It has been determined experimentally that Ni-MOF-74 is somewhat more water stable than the Mg-MOF-74.³² In addition, Jiao et al.³³ observed that a small amount of Ni doping into Mg-MOF-74 can increase the percentage of surface area retained after water exposure compared to that of pure Mg-MOF-74. Density functional theory calculations demonstrate that H₂O molecules bind more strongly with Mg (73.2 kJ/mol) open metal sites than with Ni (60.6 kJ/mol).³⁴ This persistent difference is confirmed by our thermodynamic results and 39.5 kJ/mol energetic difference between two MOFs indicates the higher hydrolytic stability of Ni-MOF-74 compared to its magnesium counterpart.

Based on molecular dynamic simulations and different experimental observations, the initial stage of MOF-74 hydrolysis involves M–OH bond formation.^{12,29} This has been demonstrated by employing a reactive force field simulation for Zn-MOF-74.³⁶ Upon interaction with the active electrophilic metal centers, the dissociation of water molecules into H⁺ and OH⁻ species is influenced by the radius of the metal ion, OH⁻ combines with M²⁺ whereas H⁺ protonates the oxygen atoms on the ligand. For this reason, we have also calculated the ΔH_{r} assuming metal hydroxide as the product instead of oxide after the hydrolysis (Tables S1 and S2). The data show that ΔH_{r} is 378.7 ± 17.4 (kJ/mol of Mg) for Mg-MOF-74 and 294.0 ± 19.5 (kJ/mol of Ni) for Ni-MOF-74, showing that the hydrolysis of MOF-74 forming M(OH)₂ is even more exothermic compared to the formation of the oxide, and maintaining the difference between Mg and Ni.

A more complete picture of the thermodynamic stability of MOFs relative to hydrolysis can be obtained by combining these new results with previously published data on MOF formation enthalpies using solution calorimetry (Table 2).^{20,37–41} Compared to M-MOF-74, the ΔH_{r} of MOF plus water forming oxide and ligand is much less exothermic for a series of zinc-containing zeolitic imidazolate frameworks (ZIFs), ranging from -42 to -19.5 kJ/mol of Zn.^{37,40} This small exothermic effect, partially compensated by negative entropy terms arising from water consumption, implies the high stability of ZIFs with respect to water and indeed their

hydrolytic stability has been confirmed by numerous literature reports.⁴²

Such a large enthalpy difference (200–250 kJ/mol of M) between ZIFs + H₂O and (Mg,Ni)-MOF-74 + H₂O can be used to evaluate the magnitude of water sensitivity for different MOFs. For divalent MOs, one can find that, with increasing electronegativity of the metal atom, the stability of oxides against hydrolysis increases. The standard formation enthalpy of Mg(OH)₂ from MgO plus H₂O(l) is −37.4 kJ/mol and for Ni(OH)₂ is −14.8 kJ/mol,⁴³ hence NiO is somewhat less unstable in water than MgO. Because carboxylate MOFs are composed of M–O moieties, this trend can be simply extended to explain the hydrolytic stability of MOFs as well. Therefore, Ni-MOF-74 is less hydrolytically unstable than Mg-MOF-74. It should be noted that the large enthalpy values obtained from the thermochemical cycles are specific to the overall hydrolysis reaction indicating that these MOFs will eventually undergo hydrolysis under the presiding thermodynamic driving force, perhaps slowly at room temperature or at a much higher rate at elevated temperatures.

This methodology can be generalized to investigate the thermodynamics of condensation/polycondensation reactions of various organic molecules (aldol condensation, Claisen condensation, and so on). Note, vitally important peptide bond formation is also a condensation reaction between two amino acids with the release of water molecules and, therefore, the developed method can be also employed to analyze thermodynamics in forming higher peptides from primary amino acids.

In summary, the thermodynamic stability of two MOF-74 materials in water was experimentally analyzed using a new methodology of high-temperature drop combustion calorimetry. These results, in conjunction with the previously obtained thermochemical data for other MOFs by room temperature solution calorimetry, define a general trend of energetics, indicating that the hydrolytic stability of the MOF-74 family is thermodynamically driven and not simply a matter of kinetics. This study provides a fundamental understanding to design and synthesize MOFs with high water stability for various emerging applications.

EXPERIMENTAL METHODS

Synthesis of Mg-MOF-74. 0.712 g of Mg(NO₃)₂·6H₂O and 0.167 g of 2,5-dihydroxyterephthalic acid were dissolved in a mixture of 67.5 mL of dimethylformamide (DMF), 4.5 mL of ethanol, and 4.5 mL of water under sonication in a 250 mL screw cap jar. The reaction jar was capped tightly and heated in an oven at 125 °C for 26 h. After cooling to room temperature, the solvent was carefully decanted from the product and replaced with methanol. The solvent exchange was carried out six times over the next three days. The solvent was removed in a dynamic vacuum at 220 °C for 12 h.

Synthesis of Ni-MOF-74. 0.602 g of Ni(NO₃)₂·6H₂O and 0.12 g of 2,5-dihydroxyterephthalic acid were dissolved in a mixture of 45 mL of DMF, 3 mL of ethanol, and 3 mL of water under sonication in a 250 mL screw cap jar. The reaction jar was capped tightly and heated in an oven at 110 °C for 60 h. After cooling to room temperature, the solvent was carefully decanted from the product and replaced with methanol. The solvent exchange was carried out six times over the next three days. The solvent was removed in a dynamic vacuum at 220 °C for 12 h.

Characterization. The crystal structure and purity of MOFs were characterized by PXRD with a Bruker D8 (AXS) Advance diffractometer, employing Ni-filtered Cu K α radiation at 40 kV and a detector current of 40 mA. The N₂ sorption experiments were performed using a Micromeritics ASAP 2020 instrument at 77 K and specific surface areas were calculated from the BET equation. Prior to gas sorption experiments, the powders were degassed at 493 K overnight under 10^{−6} Torr vacuum. The TGA was conducted using a Labsys evo Setaram instrument at a ramping rate of 10 °C/min in a 30 mL/min oxygen flow.

High-Temperature Drop Combustion Calorimetry. The drop combustion enthalpies (ΔH_{com}) of MOFs were obtained with a Calvet-type twin calorimeter (AlexSYS Setaram Inc.) in an empty quartz crucible under continuous 70 mL min^{−1} oxygen flow at 800 °C. To prepare the dropping pellets, the MOF samples were degassed at 220 °C for 12 h under 10^{−6} Torr vacuum to remove the adsorbed water. Then, the sample containing a sealed tube was transferred into an Ar-filled glove box with <1 ppm H₂O and O₂ concentration, respectively. It is very important to use completely dehydrated MOF samples because a small amount of adsorbed water can affect the combustion reaction. Because of the low density of MOFs, for each experiment around 2 mg of the samples were weighed inside the glove box using a microbalance with an accuracy of 1 μ g. Subsequently, the weighed pellets were placed inside the specially designed 3D printed dropper, which allows transferring the sample from the glove box to the calorimeter without exposing samples to air. For each sample, 4–6 dropping measurements were conducted and an average value was used for the thermodynamic calculations. The heat effect of benzoic acid was used to determine the calibration factor of the instrument.

ASSOCIATED CONTENT

Supporting Information

The Supporting Information is available free of charge at <https://pubs.acs.org/doi/10.1021/acsomega.0c01189>.

TGA curves and thermochemical tables (PDF)

AUTHOR INFORMATION

Corresponding Author

Alexandra Navrotsky – Peter A. Rock Thermochemistry Laboratory and NEAT ORU, University of California at Davis, Davis, California 95616, United States; School of Molecular Sciences and Center for Materials of the Universe, Arizona State University, Tempe, Arizona 85287, United States; orcid.org/0000-0002-3260-0364; Email: Alexandra.Navrotsky@asu.edu

Authors

Albert A. Voskanyan – Peter A. Rock Thermochemistry Laboratory and NEAT ORU, University of California at Davis, Davis, California 95616, United States; School of Molecular Sciences and Center for Materials of the Universe, Arizona State University, Tempe, Arizona 85287, United States; orcid.org/0000-0001-5639-2590

Vitaliy G. Goncharov – Department of Chemistry and Alexandra Navrotsky Institute for Experimental Thermodynamics, Washington State University, Pullman, Washington 99164, United States

Novendra Novendra – Peter A. Rock Thermochemistry Laboratory and NEAT ORU, University of California at Davis, Davis, California 95616, United States; orcid.org/0000-0003-0927-5759

Xiaofeng Guo – Department of Chemistry and Alexandra Navrotsky Institute for Experimental Thermodynamics, Washington State University, Pullman, Washington 99164, United States; orcid.org/0000-0003-3129-493X

Complete contact information is available at:
<https://pubs.acs.org/10.1021/acsomega.0c01189>

Notes

The authors declare no competing financial interest.

ACKNOWLEDGMENTS

This work was supported by the U.S. Department of Energy Office of Science, Office of Basic Energy Sciences, grant DE-FG02-03ER46053. X.G. and V.G.G. acknowledge the WSU institutional funds, facility support from the Nuclear Science Center at WSU, and support from the U.S. Department of Energy, Office of Nuclear Energy, grant DE-NE0008582. We additionally thank Dr. Qiang Zhang and Jiahong Li at WSU for assistance in using the adsorption analyzer and the glovebox for handling the MOF samples and droppers.

REFERENCES

- (1) Long, J. R.; Yaghi, O. M. Pervasive Chemistry of Metal–Organic Frameworks. *Chem. Soc. Rev.* **2009**, *38*, 1213–1214.
- (2) Zhou, H.-C.; Long, J. R.; Yaghi, O. M. Introduction to Metal–organic Frameworks. *Chem. Rev.* **2012**, *112*, 673–674.
- (3) Furukawa, H.; Cordova, K. E.; O’Keeffe, M.; Yaghi, O. M. The Chemistry and Applications of Metal–Organic–Frameworks. *Science* **2013**, *341*, 1230444.
- (4) Yaghi, O. M.; O’Keeffe, M.; Ockwig, N. W.; Chae, H. K.; Eddaoudi, M.; Kim, J. Reticular synthesis and the design of new materials. *Nature* **2003**, *423*, 705–714.
- (5) Wilmer, C. E.; Leaf, M.; Lee, C. Y.; Farha, O. K.; Hauser, B. G.; Hupp, J. T.; Snurr, R. Q. Large-scale screening of hypothetical metal–organic frameworks. *Nat. Chem.* **2012**, *4*, 83–89.
- (6) Lee, J.; Farha, O. K.; Roberts, J.; Scheidt, K. A.; Nguyen, S. T.; Hupp, J. T. Metal–organic framework materials as catalysts. *Chem. Soc. Rev.* **2009**, *38*, 1450–1459.
- (7) Kreno, L. E.; Leong, K.; Farha, O. K.; Allendorf, M.; Van Duyne, R. P.; Hupp, J. T. Metal–Organic Framework Materials as Chemical Sensors. *Chem. Rev.* **2012**, *112*, 1105–1125.
- (8) He, Y.; Zhou, W.; Qian, G.; Chen, B. Methane storage in metal–organic frameworks. *Chem. Soc. Rev.* **2014**, *43*, 5657–5678.
- (9) Wu, M.-X.; Yang, Y.-W. Metal–Organic Framework (MOF)-Based Drug/Cargo Delivery and Cancer Therapy. *Adv. Mater.* **2017**, *29*, 1606134.
- (10) Wu, H. B.; Lou, X. W. Metal–organic frameworks and their derived materials for electrochemical energy storage and conversion: Promises and challenges. *Sci. Adv.* **2017**, *3*, No. eaap9252.
- (11) Schoencker, P. M.; Carson, C. G.; Jasuja, H.; Flemming, C. J. J.; Walton, K. S. Effect of Water Adsorption on Retention of Structure and Surface Area of Metal–Organic Frameworks. *Ind. Eng. Chem. Res.* **2012**, *51*, 6513–6519.
- (12) Burtch, N. C.; Jasuja, H.; Walton, K. S. Water Stability and Adsorption in Metal–Organic Frameworks. *Chem. Rev.* **2014**, *114*, 10575–10612.
- (13) Wang, C.; Liu, X.; Keser Demir, N.; Chen, J. P.; Li, K. Applications of water stable metal–organic frameworks. *Chem. Soc. Rev.* **2016**, *45*, 5107–5134.
- (14) Bosch, M.; Zhang, M.; Zhou, H.-C. Increasing the Stability of Metal–Organic Frameworks. *Adv. Chem.* **2014**, *2014*, 1–8.
- (15) Zhang, J.-P.; Zhang, Y.-B.; Lin, J.-B.; Chen, X.-M. Metal Azolate Frameworks: From Crystal Engineering to Functional Materials. *Chem. Rev.* **2012**, *112*, 1001–1033.
- (16) Taylor, J. M.; Vaidhyanathan, R.; Iremonger, S. S.; Shimizu, G. K. H. Enhancing Water Stability of Metal–Organic Frameworks via Phosphonate Monoester Linkers. *J. Am. Chem. Soc.* **2012**, *134*, 14338–14340.
- (17) Mason, J. A.; Sumida, K.; Herm, Z. R.; Krishna, R.; Long, J. R. Evaluating metal–organic frameworks for post-combustion carbon dioxide capture via temperature swing adsorption. *Energy Environ. Sci.* **2011**, *4*, 3030–3040.
- (18) Wang, Q.; Bai, J.; Lu, Z.; Pan, Y.; You, X. Finely tuning MOFs towards high-performance post-combustion CO₂ capture materials. *Chem. Commun.* **2016**, *52*, 443–452.
- (19) Hughes, J. T.; Navrotsky, A. MOF-5: Enthalpy and Energy Landscape of Porous Materials. *J. Am. Chem. Soc.* **2011**, *133*, 9184–9187.
- (20) Hughes, J. T.; Sava, D. F.; Nenoff, T. M.; Navrotsky, A. Thermochemical Evidence for Strong Iodine Chemisorption by ZIF-8. *J. Am. Chem. Soc.* **2013**, *135*, 16256–16259.
- (21) Huskić, I.; Novendra, N.; Lim, D.-W.; Topic, F.; Titi, H. M.; Pekov, I. V.; Krivovichev, S. V.; Navrotsky, A.; Kitagawa, H.; Friscic, T. Functionality in metal–organic framework minerals: proton conductivity, stability and potential for polymorphism. *Chem. Sci.* **2019**, *10*, 4923–4929.
- (22) Guo, X.; Boukhalfa, H.; Mitchell, J. N.; Ramos, M.; Gaunt, A. J.; Migliori, A.; Roback, R. C.; Navrotsky, A.; Xu, H. Sample seal-and-drop device and methodology for high temperature oxide melt solution calorimetric measurements of PuO₂. *Rev. Sci. Instrum.* **2019**, *90*, 044101.
- (23) Rosi, N. L.; Kim, J.; Eddaoudi, M.; Chen, B.; O’Keeffe, M.; Yaghi, O. M. Rod Packings and Metal–Organic Frameworks Constructed from Rod-Shaped Secondary Building Units. *J. Am. Chem. Soc.* **2005**, *127*, 1504–1518.
- (24) Sun, H.; Ren, D.; Kong, R.; Wang, D.; Jiang, H.; Tan, J.; Wu, D.; Chen, S.; Shen, B. Tuning 1-hexene/n-hexane adsorption on MOF-74 via constructing Co–Mg bimetallic frameworks. *Microporous Mesoporous Mater.* **2019**, *284*, 151–160.
- (25) Chen, C.; Feng, X.; Zhu, Q.; Dong, R.; Yang, R.; Cheng, Y.; He, C. Microwave-Assisted Rapid Synthesis of Well-Shaped MOF-74 (Ni) for CO₂ Efficient Capture. *Inorg. Chem.* **2019**, *58*, 2717–2728.
- (26) Caskey, S. R.; Wong-Foy, A. G.; Matzger, A. J. Dramatic Tuning of Carbon Dioxide Uptake via Metal Substitution in a Coordination Polymer with Cylindrical Pores. *J. Am. Chem. Soc.* **2008**, *130*, 10870–10871.
- (27) Yang, D.-A.; Cho, H.-Y.; Kim, J.; Yang, S.-T.; Ahn, W.-S. CO₂ capture and conversion using Mg–MOF-74 prepared by a sonochemical method. *Energy Environ. Sci.* **2012**, *5*, 6465–6473.
- (28) Kizzie, A. C.; Wong-Foy, A. G.; Matzger, A. J. Effect of Humidity on the Performance of Microporous Coordination Polymers as Adsorbents for CO₂ Capture. *Langmuir* **2011**, *27*, 6368–6373.
- (29) Tan, K.; Zuluaga, S.; Gong, Q.; Canepa, P.; Wang, H.; Li, J.; Chabal, Y. J.; Thonhauser, T. Water Reaction Mechanism in Metal Organic Frameworks with Coordinatively Unsaturated Metal Ions: MOF-74. *Chem. Mater.* **2014**, *26*, 6886–6895.
- (30) Zuluaga, S.; Fuentes-Fernandez, E. M. A.; Tan, K.; Xu, F.; Li, J.; Chabal, Y. J.; Thonhauser, T. Understanding and controlling water stability of MOF-74. *J. Mater. Chem. A* **2016**, *4*, 5176–5183.
- (31) Kumar, A.; Madden, D. G.; Lusi, M.; Chen, K.-J.; Daniels, E. A.; Curtin, T.; Perry, J. J.; Zaworotko, M. J. Direct Air Capture of CO₂ by Physisorbent Materials. *Angew. Chem., Int. Ed.* **2015**, *54*, 14372–14377.
- (32) Liu, J.; Benin, A. I.; Furtado, A. M. B.; Jakubczak, P.; Willis, R. R.; Levan, M. D. Stability Effects on CO₂ Adsorption for the DOBDC Series of Metal–Organic Frameworks. *Langmuir* **2011**, *27*, 11451–11456.
- (33) Jiao, Y.; Morelock, C. R.; Burtch, N. C.; Mounfield, W. P.; Hungerford, J. T.; Walton, K. S. Tuning the Kinetic Water Stability

and Adsorption Interactions of Mg-MOF-74 by Partial Substitution with Co or Ni. *Ind. Eng. Chem. Res.* **2015**, *54*, 12408–12414.

(34) Canepa, P.; Arter, C. A.; Conwill, E. M.; Johnson, D. H.; Shoemaker, B. A.; Soliman, K. Z.; Thonhauser, T. High-throughput screening of small-molecule adsorption in MOF. *J. Mater. Chem. A* **2013**, *1*, 13597–13604.

(35) Robie, R. A.; Hemingway, B. S. Thermodynamic Properties of Minerals and Related Substances at 298.15 K and 1 Bar (10^5 Pascals) Pressure and at Higher Temperatures, *US Geological Survey Bulletin*, 2131; US Government Printing Office, 1995.

(36) Han, S. S.; Choi, S.-H.; van Duin, A. C. T. Molecular dynamics simulations of stability of metal–organic frameworks against H₂O using the ReaxFF reactive force field. *Chem. Commun.* **2010**, *46*, 5713–5715.

(37) Hughes, J. T.; Bennett, T. D.; Cheetham, A. K.; Navrotsky, A. Thermochemistry of Zeolitic Imidazolate Frameworks of Varying Porosity. *J. Am. Chem. Soc.* **2013**, *135*, 598–601.

(38) Wu, D.; Navrotsky, A. Thermodynamics of metal-organic frameworks. *J. Solid State Chem.* **2015**, *223*, 53–58.

(39) Akimbekov, Z.; Wu, D.; Brozek, C. K.; Dincă, M.; Navrotsky, A. Thermodynamics of solvent interaction with the metal-organic framework MOF-5. *Phys. Chem. Chem. Phys.* **2016**, *18*, 1158–1162.

(40) Akimbekov, Z.; Katsenis, A. D.; Nagabhushana, G. P.; Ayoub, G.; Arhangelskis, M.; Morris, A. J.; Friščić, T.; Navrotsky, A. Experimental and Theoretical Evaluation of the Stability of True MOF Polymorphs Explains Their Mechanochemical Interconversions. *J. Am. Chem. Soc.* **2017**, *139*, 7952–7957.

(41) Arhangelskis, M.; Katsenis, A. D.; Novendra, N.; Akimbekov, Z.; Gandrath, D.; Marrett, J. M.; Ayoub, G.; Morris, A. J.; Farha, O. K.; Friščić, T.; Navrotsky, A. Theoretical Prediction and Experimental Evaluation of Topological Landscape and Thermodynamic Stability of a Fluorinated Zeolitic Imidazolate Framework. *Chem. Mater.* **2019**, *31*, 3777–3783.

(42) Park, K. S.; Ni, Z.; Cote, A. P.; Choi, J. Y.; Huang, R.; Uribe-Romo, F. J.; Chae, H. K.; O’Keeffe, M.; Yaghi, O. M. Exceptional chemical and thermal stability of zeolitic imidazolate frameworks. *Proc. Natl. Acad. Sci. U.S.A.* **2006**, *103*, 10186–10191.

(43) Allada, R. K.; Peltier, E.; Navrotsky, A.; Casey, W. H.; Johnson, C. A.; Berbeco, H. T.; Sparks, D. L. Calorimetric determination of the enthalpies of formation of hydrotalcite-like solids and their use in the geochemical modeling of metals in natural waters. *Clays Clay Miner.* **2006**, *54*, 409–417.